Hindawi
International Journal of Polymer Science
Volume 2024, Article ID 2723981, 9 pages
https://doi.org/10.1155/2024/2723981

Research Article

Preparation and Characterization of Thermally Conductive High Impact Polystyrene/AlN Composite

Nghiem Thi Thuong, Nguyen Ba Lam, Pham Anh Son, Nguyen Ba Chien, Nguyen Pham Duy Linh, Chu Thi Hai Nam, and Nguyen Anh Vu

Hanoi University of Science and Technology, No 1 Dai Co Viet, Hanoi 10000, Vietnam

Correspondence should be addressed to Nghiem Thi Thuong; thuong.nghiemthi@hust.edu.vn and Nguyen Anh Vu; vu.nguyenanh@hust.edu.vn

Received 25 October 2023; Revised 30 November 2023; Accepted 10 January 2024; Published 19 January 2024

Academic Editor: Antonio Caggiano

In the present work, AlN was modified with vinyltriethoxysilane (VTES), and its effect on the properties of a thermally conductive composite of high impact polystyrene (HIPS), and AlN was investigated. Three composites, HIPS/AlN5, HIPS/AlN9, and HIPS/moAlN9, were prepared by mixing HIPS and AlN in a toluene solution, followed by hot pressing. The HIPS/AlN composite was characterized by tensile test, impact strength, flexural strength, and hardness shore D. The sample HIPS/moAlN9 showed the improvement of these properties compared to that of the HIPS/AlN9 sample. The increment of those mechanical properties was due to the good interaction between the modified AlN and HIPS resin matrix, which was revealed by morphology observation by SEM. Incorporating modified AlN into the HIPS matrix was also found to enhance the thermal conductivity by about 20%, from 0.15 for HIPS to 0.18 (W/m·K) for HIPS/moAlN9. It was explained due to the good adherence of AlN to the HIPS, which provided more thermal conductive routes than HIPS/AlN. This approach provides a possible strategy to prepare thermally conductive HIPS composite, which may be suitable for electronic device that required heat dissipation.

1. Introduction

Since the introduction of the first plastic, Bakelite, by Leo Baekeland in 1907, the world has experienced a revolutionary advancement in plastics [1]. Plastic materials find extensive applications across various industrial sectors and the consumer goods industry [2–4]. Notably, one of the most significant areas where plastics have made a remarkable impact is in serving as materials for electrical devices [5–7]. However, many polymeric materials exhibit thermal insulating properties, with thermal conductivity typically ranging from 0.1 to 0.5 W/m·K. This inherent insulating behavior has led to widespread use of plastics in numerous parts of electrical devices. Yet, their thermal insulating nature poses limitations on their applications, potentially resulting in increased temperatures within devices and compromising the overall performance of electrical systems [8, 9].

The most common method to enhance the thermal conductivity of plastics involves the addition of thermally conductive fillers. These fillers typically include carbon-based additives such as graphene, carbon nanotubes, carbon fibers [10–13], metals [14–16], and metal oxides [17, 18]. Additionally, aluminum nitride (AlN) has emerged as a promising and effective filler in thermally conductive composites used in electrical devices due to its exceptional thermal conductivity, high electrical resistivity, and cost-effectiveness. When utilized as a thermally conductive filler, AlN is often modified with a silane coupling agent to optimize its interaction with the polymer matrix. For example, Zhou et al. successfully fabricated thermally conductive polypropylene/AlN composites by incorporating octyltriethoxysilane-functionalized AlN nanoparticles [19]. In another study conducted by Lule and Kim, the thermal conductivity of poly (butylene succinate)/AlN composites was investigated, highlighting the superior effectiveness of vinyltriethoxylsilane

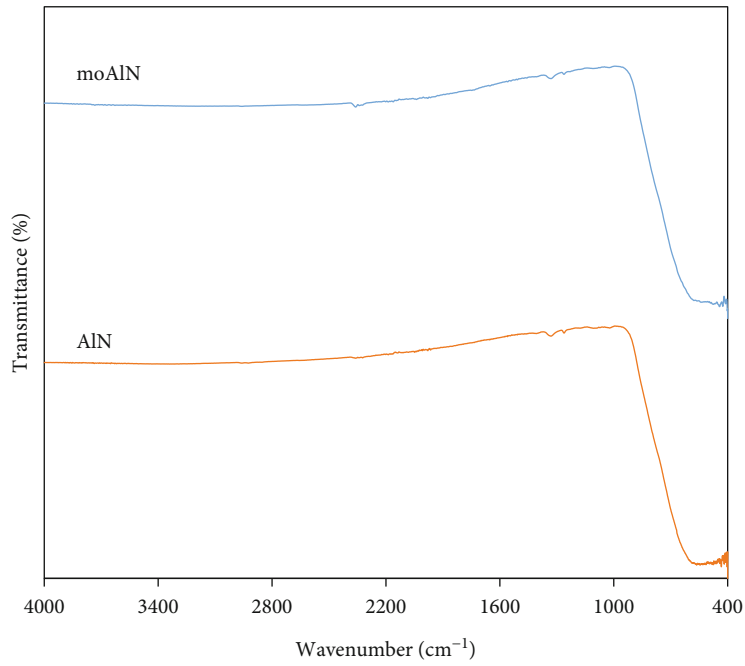

Figure 1: FTIR spectra of AlN and modified AlN.

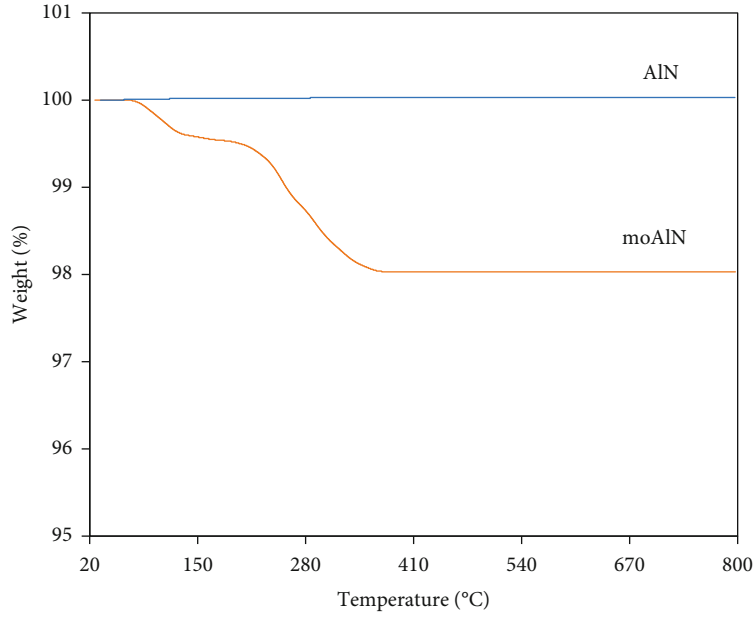

Figure 2: TGA diagram of AlN and modified AlN.

(VTES) as a surface modification agent for AlN particles compared to other types of silane coupling agents [20].

High impact polystyrene (HIPS), a member of the polystyrene family, offers versatility by combining favorable polystyrene traits with exceptional impact resistance. Its broad range of applications [21, 22] includes its use in electronic devices, particularly for electrical insulation and consumer electronics accessories. However, HIPS demonstrates relatively low thermal conductivity, measuring only 0.1 W/m·K at room temperature [23, 24]. Furthermore, its thermal conductivity exhibits minimal increase with rising temperatures [25]. Recent research efforts aimed at enhancing the thermal conductivity of HIPS have explored various strategies [26–28], such as incorporating metal alloys. For instance, Yu et al. investigated the use of Cu alloys to improve HIPS' thermal conductivity [24]. While the results showed consistent thermal conductivity regardless of temperature, an increase in Cu alloy content up to 70% was found to potentially compromise the dielectric properties of HIPS, posing a risk of electrical applications being affected.

➢ Surface modification of AlN with vinyltriethoxysilane

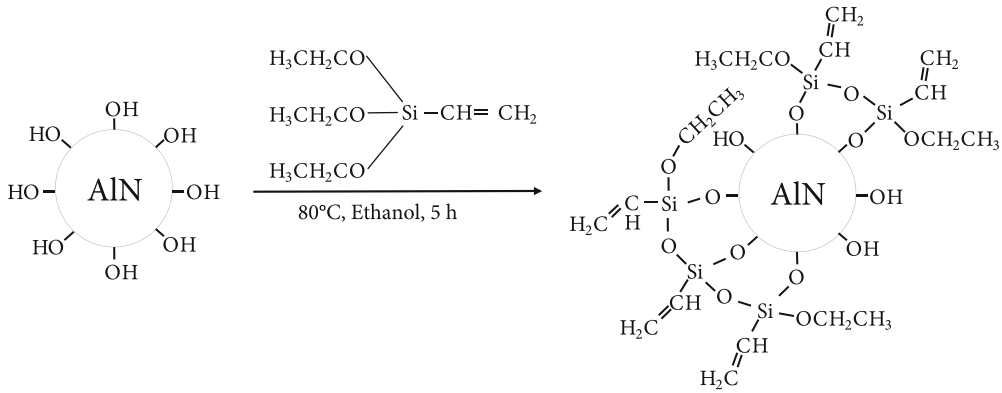

➢ Solution mixing of AlN and moAlN particles in Toluene/HIPS solution

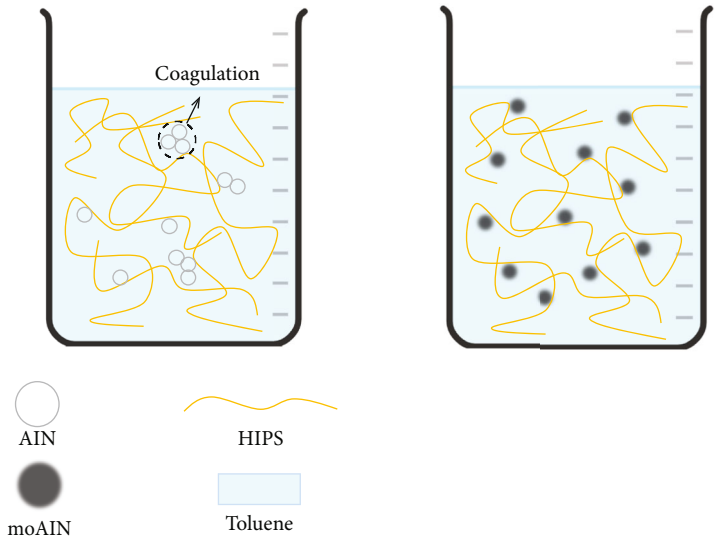

Figure 3: Modification of AlN and preparation of HIPS/AlN composite.

The objective of this study was to enhance the thermal conductivity of HIPS while maintaining its mechanical properties by integrating AlN as a filler. HIPS/AlN composites were synthesized through a solution mixing method, followed by a comprehensive characterization encompassing evaluations of both thermal conductivity and mechanical properties. The surface modification of AlN particles was conducted using VTES to improve the interaction between the plastic matrix and the filler. To the author's knowledge, no previous studies have investigated or reported on thermally conductive HIPS/AlN composites.

2. Materials and Methods

2.1. Materials. The resin matrix used in this work is high impact polystyrene plastic beads (Styrolution PS 476 L) that were supplied from Styrolution, Germany. Aluminum nitride particles as a thermally conductive filler with an average size of 10 μm and purity of 99.9% were provided from Aladdin Industrial Corporation, China. Vinyltriethoxysilane as a silane coupling agent with a purity of 97%, ethanol as a solvent for modification (95%), and toluene (99.7%) as a casting solvent were purchased from Sigma-Aldrich, Germany.

Table 1: Composition of HIPS/AlN composites.

Samples	HIPS (phr)	AlN (phr)	moAlN (phr)
HIPS	100	—	—
HIPS/AlN5	100	5	—
HIPS/AlN9	100	9	—
HIPS/moAlN9	100	—	9

2.2. Surface Modification of AlN Particle. Firstly, the AlN particles were dispersed in ethanol by ultrasonicating for 30 minutes before pouring into a two-neck flask. Then, 10 wt% of VTES (based on the weight of AlN particles) were added to the mixtures in the two-neck flask. The modification was carried out by stirring the mixture at 80°C for 5 hours. After that, the modified AlN was centrifuged at

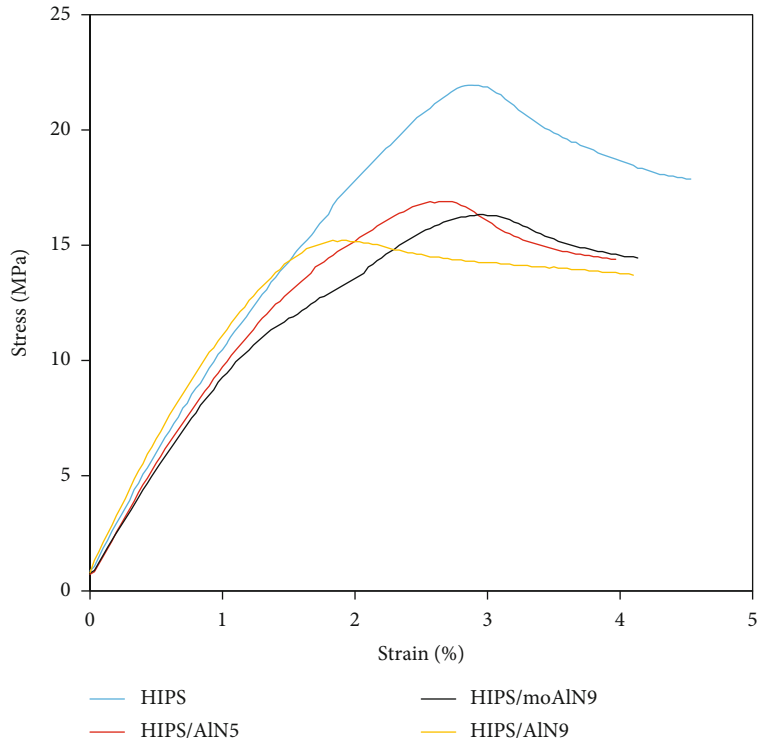

Figure 4: Tensile strength of HIPS and HIPS/AlN composites.

10,000 rpm for 15 minutes three times to remove unreacted VTES. Finally, modified AlN (moAlN) was placed in an oven and dried at 50°C to remove residual solvent.

2.3. Preparation of Thermally Conductive Composites. HIPS/AlN and HIPS/moAlN composites were fabricated by using the solution mixing method with toluene as a casting solvent. HIPS pellets were dried in a desiccator at 80°C for 4 hours to remove any residual moisture. AlN and moAlN were dispersed in toluene by stirring and sonicating for 30 minutes each. Then, HIPS pellets were slowly added under continuous stirring. This process was completed after the HIPS pellets were fully dissolved. The mixture then was poured on stainless steel trays and dried completely. Then, it was cut into small pieces. The amount of AlN in the composites used was 0, 5, and 9 phr, and that of modified AlN was 9 phr.

To prepare the film for mechanical and thermal testing, the composite samples were pressed with hot pressing at 180°C under a pressure of 20 MPa in 10 minutes. The samples, after that, were cooled to the room temperature while keeping at the same pressure. The film was prepared with a thickness of 3 mm.

2.4. Characterizations. Fourier-transform infrared spectroscopy (FTIR) measurement of AlN and moAlN was carried out with a Thermo Scientific Nicolet iS50 FTIR spectrometer at 100 scans, with wavelengths ranging from 400 cm^{-1} to 4000 cm^{-1}, and a resolution of 4 cm^{-1}.

Thermal gravimetric analysis (TGA) of the AlN and moAlN particles was performed on a TA Q500 instrument at a heating rate of 10°C/min from room temperature to 800°C in a nitrogen atmosphere. The weight of AlN and moAlN used for TGA measurement was 10 mg and 60 mg, respectively.

Table 2: Impact strength, flexural strength, and hardness shore D of HIPS/AlN composites.

Samples	Impact strength (kJ/m^2)	Flexural strength (MPa)	Hardness shore D
HIPS	8.074	75.28	74.64 ± 0.19
HIPS/AlN5	8.703	58.12	71.88 ± 0.38
HIPS/AlN9	8.857	60.23	70.63 ± 0.38
HIPS/moAlN9	9.626	62.93	72.13 ± 0.19

The thermal conductivity (λ, W/m·K) measurement method is based on the principle of determining the temperature gradient and heat flux through the object to be measured using a heat flow meter. The measuring system includes two FHF25C series heat flux sensors: HUKSEFLEX, Memory Hilogger LR8450—HIOKI—and PMC-18-5A, Compact Low Noise Linear DC Power Supply—KIKUSUI.

Tensile strength was determined according to ASTM D638 on the INSTRON 5582-100 kN Universal Mechanical Testing machine with a 20 mm/min test speed.

The flexural strength was determined according to the international standard ISO 178:1993, measured on a Lloyd LRX Plus Materials Testing Machine with a 20 mm/min bending speed.

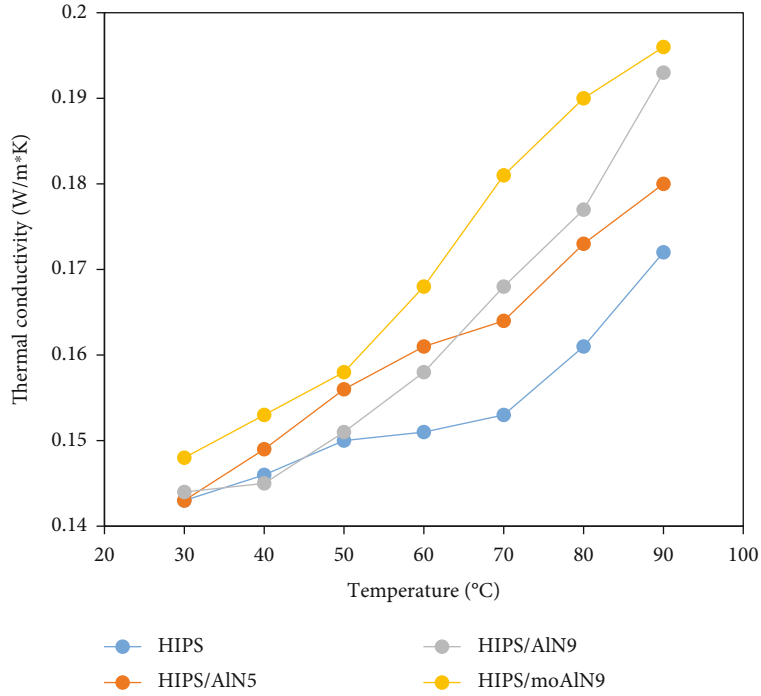

Figure 5: Thermal conductivity of HIPS and HIPS/AlN.

The izod impact strength was determined on a Tinius Olsen Plastic Pendulum Impact Tester IT504 machine (USA) according to ASTM D256–06.

Shore D hardness was measured by Shore D Durometer Hardness Tester HT-6600D.

Scanning electron microscope (SEM) analysis of the sample was observed by field emission scanning microscopy (FE-SEM) with JEOL JSM 7600 (USA). The sample was fractured, and the fracture surface was observed.

Energy dispersive analysis (EDX) mapping of elements in the samples was carried out with the FE-SEM system HITACHI S-4800. The accelerating voltage is 20 kV.

Table 3: Thermal conductivity of HIPS/AlN composites.

Temp. (°C)	Thermal conductivity (W/m.K)			
	HIPS	HIPS/AlN5	HIPS/AlN9	HIPS/moAlN9
30	0.143	0.143	0.144	0.148
40	0.146	0.149	0.145	0.153
50	0.150	0.156	0.151	0.158
60	0.151	0.161	0.158	0.168
70	0.153	0.164	0.168	0.181
80	0.161	0.173	0.177	0.190
90	0.172	0.180	0.193	0.196

3. Results and Discussion

3.1. Modification of AlN. ATR-FTIR spectroscopy was utilized to characterize the surface of AlN particles before and after modification. Figure 1 depicts the ATR-FTIR spectra for AlN and moAlN. In the FTIR spectra for AlN, a fundamental vibration that appeared at 675 cm^{-1} was attributed to AlN. Additionally, no significant differences are evident in the FTIR spectra between raw and moAlN nanoparticles. This observation suggests that there might not have been the formation of new functional groups on AlN after modification. However, earlier studies propose that this lack of significant change could be attributed to the formation of only a small amount of hydrolyzed VTES on AlN [25]. Consequently, further investigation into the formation of hydrolyzed VTES was conducted using TGA and SEM/EDX.

Figure 2 displays the TGA curves of AlN and moAlN. The TGA curve for AlN indicates no significant weight loss across all temperatures. On the other hand, the TGA curve for moAlN exhibited a two-step weight loss pattern. The initial step involved the loss of absorbed moisture at lower temperatures, followed by the subsequent loss of organic groups attached to the AlN particle surface at higher temperatures. The weight loss observed in moAlN particles accounts for approximately 2 wt%, corresponding to the removal of VTES introduced during surface modification. These TGA results further support the successful grafting of the silane coupling agent onto the surface of the AlN particle as proposed in Figure 3.

3.2. Characterization of HIPS/AlN Composite. Table 1 shows the composition of HIPS/AlN composites. Three HIPS/AlN composites were prepared with 5 phr, 9 phr of raw AlN, and 9 phr of modified AlN. The control sample, HIPS resin, was also prepared. The mechanical properties of these composites were characterized, and the morphology was observed.

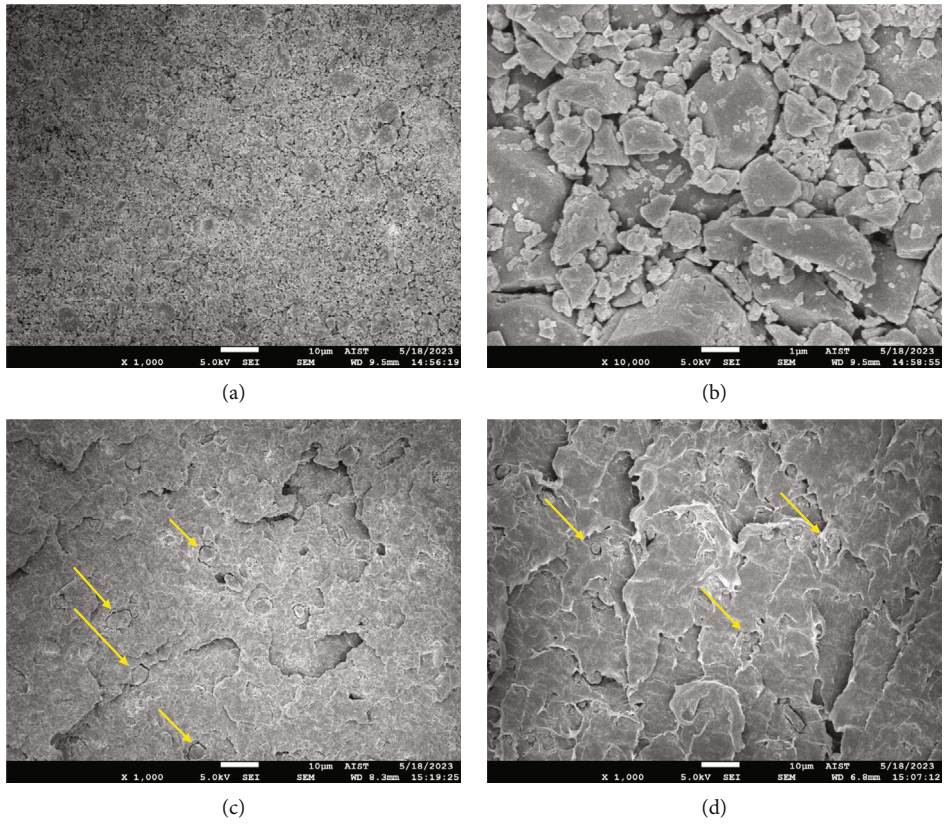

Figure 6: SEM images of (a) AlN powder at 1,000 magnification and (b) at 10,000 magnifications and (c) HIPS/AlN and (d) HIPS/moAlN at 1,000 magnification.

Figure 4 shows the stress-strain curves for the HIPS, HIPS/AlN5, HIPS/AlN9, and HIPS/moAlN. As shown in Figure 4, the ultimate tensile strength of the HIPS sample was 22.0 MPa. This value decreased to 17.0 MPa for HIPS/AlN5 and 15.2 MPa for HIPS/AlN9. It suggests that loading with AlN particles decreased the ultimate tensile strength of HIPS resin. It may be due to the lack of interaction between the AlN filler and the HIPS matrix. Poor interaction of AlN and HIPS may be resulted in disconnection between the AlN filler in the HIPS matrix. After modification of AlN with VTES, the ultimate strength of HIPS/moAlN9 was about 16.3 MPa, which was a little higher than that for HIPS/AlN composite. This slight improvement may be attributed to the functionalization of the AlN surface with VTES. The vinyl group, -CH=CH_2, in the AlN surface may increase the hydrophobicity of AlN particles. Therefore, modified AlN may have interacted better with HIPS resin compared to raw AlN.

Table 2 shows the impact strength, flexural strength, and hardness of HIPS, HIPS/AlN5, HIPS/AlN9, and HIPS/moAlN. The impact strength of HIPS increased as increasing AlN loading. The increase in impact strength for HIPS/AlN composites demonstrated that the composites have a better resistance to fractureness under stress at high speed of testing. It is essential for the application of the HIPS/AlN composite. The sample HIPS/moAlN9 composite prepared with modified AlN shows the highest impact strength that is 9.626 kJ/m^2. The increase in impact strength for HIPS/moAlN9 suggests a better interaction between the modified AlN and HIPS matrix.

In contrast to impact strength, the flexural strength of the HIPS/AlN5 and HIPS/AlN9 is 58.12 MPa and 60.23 MPa, respectively. This value decreased compared to that of HIPS (75.28 MPa). However, the flexural strength improved a little to 62.93 MPa for HIPS/moAlN. As can be seen, the flexural strength slightly increased with increasing AlN loading. This property is completely distinguished from the tensile strength, in which the higher the AlN loading, the poorer the tensile strength. It was noted that HIPS/moAlN achieved high tensile strength, impact strength, and flexural strength among the samples. It suggested that modifying AlN increased the compatibility for the AlN with the HIPS matrix. This observation is consistent with the literature that good dispersion of filler in resin matrix resulted in better performance of the tensile strength and the flexural strength [29–31]. It may confirm that the dispersion of AlN in the HIPS matrix is more improved after AlN was modified with VTES.

The HIPS/AlN composites were subjected to a hardness test with shore D type. The hardness of the composites is the ability of materials to withstand force without deformation and indentation. As shown in Table 2, the hardness value for HIPS was 74.64, and those for HIPS/AlN5 and HIPS/AlN9 were 71.88 and 70.63, respectively. The hardness of the HIPS/AlN composite was found to decrease when increasing AlN loading. However, the hardness of HIPS/

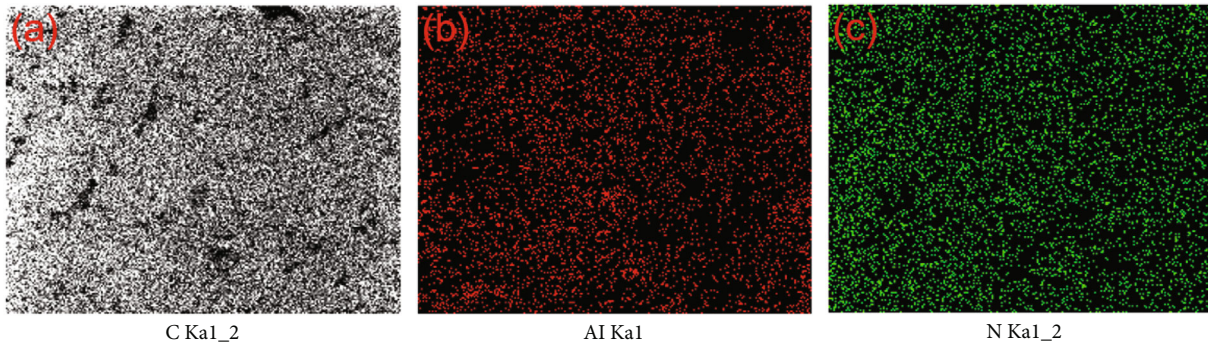

Figure 7: EDX mapping for HIPS/AlN9 (a) C map, (b) Al map, and (c) N map.

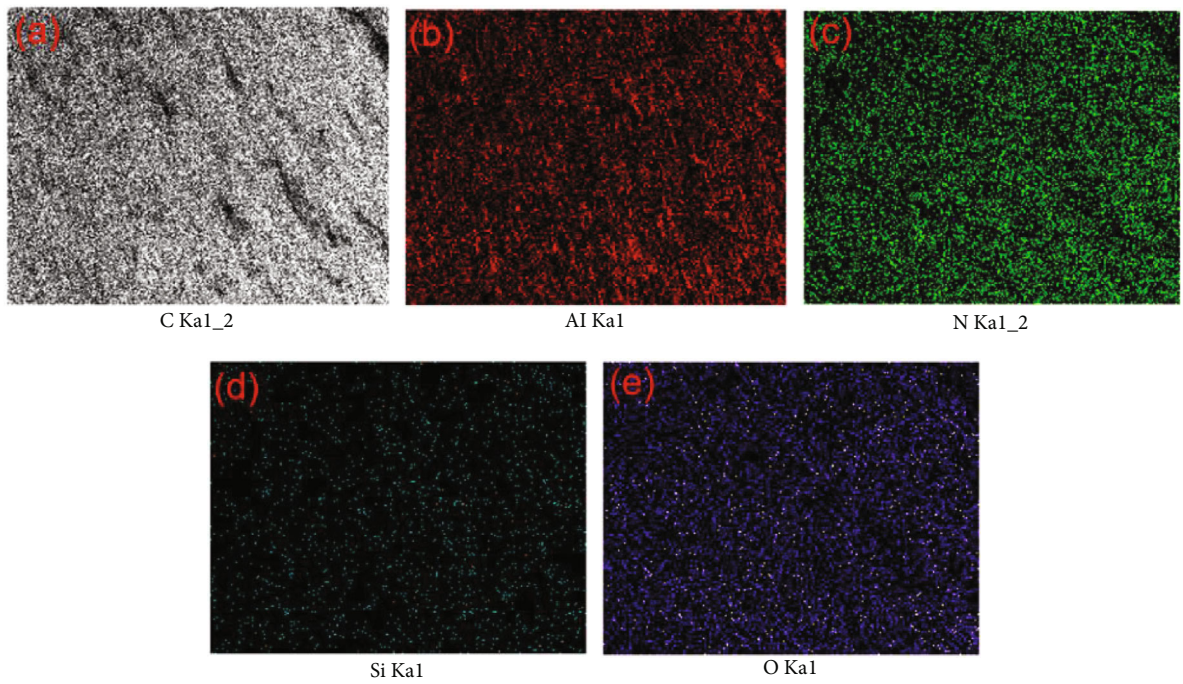

Figure 8: EDX mapping for HIPS/moAlN9 (a) C map, (b) Al map, (c) N map, (d) Si map, and (e) O map.

moAlN increased slightly to 72.13 after AlN was modified with VTES. This result suggests that the HIPS/moAlN composite could exhibit a comparable ability to resist the deformation to that of HIPS [32, 33].

3.3. Thermal Conductivity. The heat conductivity of HIPS/AlN was characterized by measuring thermal conductivity across various temperatures, ranging from 30°C to 90°C. Figure 5 displays the thermal conductivity values of HIPS, HIPS/AlN5, HIPS/AlN9, and HIPS/moAlN9, with specific values listed in Table 3. As temperatures increased, the thermal conductivity of both HIPS and HIPS/AlN composites exhibited an upward trend. At a certain temperature, the thermal conductivity of HIPS/AlN and HIPS/moAlN composites was noticeably improved as compared to that of HIPS. It was noted that the thermal conductivity of HIPS/AlN5 was higher than that of HIPS/AlN9 at temperatures ranging from 40°C to 90°C, while it was lower thermal conductivity than HIPS/AlN5 at temperatures from 70°C to 90°C. This evidence suggested that AlN contributed to the thermal conductivity of HIPS/AlN composites. HIPS/moAlN9 exhibited the best thermal conductivity at a range of temperatures from 30°C to 90°C. This result may be attributed to better dispersion of moAlN in the HIPS matrix, leading to better thermal conductivity [34].

3.4. Morphology Observation. The distribution of AlN in the HIPS matrix is a very important indicator for enhancing the mechanical and thermal properties. Figure 6 shows the SEM images of AlN, HIPS/AlN, and HIPS/moAlN. The observed surface was prepared by fracturing the composite sample after keeping it in the freezer for several hours. The SEM image of AlN shows that AlN powder has different sizes and shapes. The size of AlN particles was about 5 μm. As can be seen in the SEM image of HIPS/AlN, the boundary between the AlN and HIPS matrix was clearly visible. It

may be explained to be due to the poor compatibility of AlN with the HIPS matrix.

In contrast, the SEM image of HIPS/moAlN showed an unclear boundary between the AlN and HIPS matrix. It was evidence of better interaction and compatibility between modified AlN and HIPS. The better interaction, the better reinforcement of AlN for the HIPS matrix. Furthermore, the better compatibility of HIPS and moAlN also provides much more effective thermal conduction pathways for the HIPS/moAlN composite, as discussed previously.

3.5. SEM/EDX Mapping. The dispersion of AlN in HIPS resin was investigated through SEM/EDX mapping. Figure 7 shows the EDX mapping of C, N, and Al elements for HIPS/AlN. The mapping of Al (Figure 7(b)) demonstrates that the dispersion of AlN in the HIPS matrix is uneven. Particularly, some parts in the images illustrate the absence of Al atoms, and the other shows the agglomeration.

Figure 8 shows the EXD mapping of C, N, Al, S, and O for HIPS/moAlN. The mapping of Al (Figure 8(b)) revealed a better dispersion of Al atoms in the HIPS/moAlN than in the HIPS/AlN sample (Figure 7(b)). It was noted that the distribution of Al atoms showed a correlation with the distribution of Si and O atoms (Figures 8(d) and 8(e)), respectively. The presence of Si and O in the EDX mapping of HIPS/AlN suggested the successful modification of AlN. The homogenous distribution of Si indicated that the modified AlN was dispersed better in the HIPS matrix than AlN. The enhancement could be attributed to the modification of AlN particles with VTES.

4. Conclusion

In this study, novel composite materials comprising HIPS and AlN were fabricated and studied for their mechanical properties and thermal conductivity. The successful modification of the AlN surface using VTES as a silanization agent was achieved. This modification notably enhanced the interaction between the moAlN particles and the HIPS matrix, resulting in an improvement of dispersion. The result demonstrated that, at a loading of 9 phr, the HIPS/AlN composites exhibited better thermal conductivity at room temperature and at higher temperatures. Moreover, the mechanical properties of HIPS/moAlN surpassed those of HIPS/AlN composites at the same filler loading. It indicated that the interaction between HIPS and the modified AlN was improved. These outcomes signify the successful creation of thermally conductive HIPS which possesses commendable mechanical properties. The result in the present work, thus, may broaden HIPS's potential applications, particularly as thermally conductive materials for electronic devices.

Data Availability

The data used to support the findings of this study are included within the article.

Conflicts of Interest

The authors declare that they have no conflicts of interest.

Acknowledgments

This research is funded by the Ministry of Industry and Trade of the Socialist Republic of Vietnam (MOIT) with grant number ĐT. CNKKQG.004/21.

References

[1] R. Geyer, "A Brief History of Plastics," in *Mare Plasticum-The Plastic Sea*, M. Streit-Bianchi, M. Cimadevila, and W. Trettnak, Eds., Springer, Cham, 2020.

[2] A. L. Andrady and M. A. Neal, "Applications and societal benefits of plastics," *Philosophical Transactions of the Royal Society B: Biological Sciences*, vol. 364, no. 1526, pp. 1977–1984, 2009.

[3] S. H. Mikael, "Chapter 26- barrier packaging materials," *Handbook of Environmental Degradation of Materials*, , William Andrew Publishingp. 559, 3rd edition, 2018.

[4] B. Kumar, A. Pundir, V. Mehta, B. Singh, and R. Chauhan, "A review paper on plastic, its variety, current scenario, and it's waste management plant," *Plant Archives*, vol. 20, pp. 53–56, 2020.

[5] J. Chunmiao, D. Pallab, K. Insup, Y. Yong-jin, T. Chor Yong, and L. Jong-Min, "Applications, treatments, and reuse of plastics from electrical and electronic equipment," *Journal of Industrial and Engineering Chemistry*, vol. 110, pp. 84–99, 2022.

[6] "Plastics for Use in Electrical Engineering," *Nature*, vol. 139, no. 3512, p. 320, 1937.

[7] A. R. Dunton and A. Caress, "Plastics for use in electrical engineering," *Journal of the Institution of Electrical Engineers*, vol. 79, no. 478, pp. 463–482, 1936.

[8] V. Lakshminarayanan and N. Sriraam, "The effect of temperature on the reliability of electronic components," in *2014 IEEE International Conference on Electronics, Computing and Communication Technologies (CONECCT)*, pp. 1–6, Bangalore, India, 2014.

[9] A. A. Adel, "The effects of heat on electronic components," *International Journal of Engineering Research and Applications*, vol. 7, no. 5, pp. 52–57, 2017.

[10] H. Jin-Ho, P. Dong-Wha, and S. Sang-Eun, "A review on thermal conductivity of polymer composites using carbon-based fillers : carbon nanotubes and carbon fibers," *Carbon Letters*, vol. 11, no. 4, pp. 347–356, 2010.

[11] A. Klemenz, L. Mayrhofer, B. Lenczowski, and M. Moseler, "Carbon nanotubes as fillers for composites with enhanced thermal conductivity," *Physical Review Materials*, vol. 5, no. 8, article 086001, 2021.

[12] H. Zhidong and F. Alberto, "Thermal conductivity of carbon nanotubes and their polymer nanocomposites: a review," *Progress in Polymer Science*, vol. 36, no. 7, pp. 914–944, 2011.

[13] B. Hung-Thang, N. Van-Chuc, P. Van-Trinh, T. N. Thi-Thanh, and P. Ngoc-Minh, "Thermal disipation media for high power electronic devices using a carbon nanotube-based composites," *Advances in Natural Sciences: Nanoscience and Nanotechnology*, vol. 2, no. 2, article 025002, 2011.

[14] S. Yu, J. W. Lee, T. H. Han et al., "Copper shell networks in polymer composites for efficient thermal conduction," *ACS*

Applied Materials & Interfaces, vol. 5, no. 22, pp. 11618–11622, 2013.

[15] L. Liang, P. Xu, Y. Wang et al., "Flexible polyvinylidene fluoride film with alternating oriented graphene/Ni nanochains for electromagnetic interference shielding and thermal management," *Chemical Engineering Journal*, vol. 395, article 125209, 2020.

[16] Z. Ma, S. Kang, J. Ma et al., "Ultraflexible and mechanically strong double-layered aramid nanofiber-$Ti_3C_2T_x$ MXene/silver nanowire nanocomposite papers for high-performance electromagnetic interference shielding," *ACS Nano*, vol. 14, no. 7, pp. 8368–8382, 2020.

[17] O. Yuge, B. Liuyang, T. Huafeng, L. Xiaofei, and Y. Fangli, "Recent progress of thermal conductive ploymer composites: Al_2O_3 fillers, properties and applications," *Composites Part A: Applied Science and Manufacturing*, vol. 152, article 106685, 2022.

[18] I. Hyungu and K. Jooheon, "Enhancement of the thermal conductivity of aluminum oxide–epoxy terminated poly (dimethyl siloxane) with a metal oxide containing polysiloxane," *Journal of Materials Science*, vol. 46, no. 20, pp. 6571–6580, 2011.

[19] Y. Zhou, J. Hu, X. Chen, F. Yu, and J. He, "Thermoplastic polypropylene/aluminum nitride nanocomposites with enhanced thermal conductivity and low dielectric loss," *IEEE Transactions on Dielectrics and Electrical Insulation*, vol. 23, no. 5, pp. 2768–2776, 2016.

[20] Z. Lule and J. Kim, "Surface modification of aluminum nitride to fabricate thermally conductive poly(butylene succinate) nanocomposite," *Polymers*, vol. 11, no. 1, p. 148, 2019.

[21] M. Martin, J. Viola, and J. Wünsch, *Preparation, Properties and Applications of High-impact Polystyrene Modern Styreneic Polymers: Polystyrene and Styrenic Copolymers*, John Wiley and Son, 2023.

[22] M. Sieradzka, J. Fabia, D. Biniaś, T. Graczyk, and R. Fryczkowski, "High-impact polystyrene reinforced with reduced graphene oxide as a filament for fused filament fabrication 3D printing," *Materials*, vol. 14, no. 22, p. 7008, 2021.

[23] W. Guilong, Z. Guoqun, D. Guiwei, S. Libin, and B. P. Chul, "Lightweight, thermally insulating, and low dielectric microcellular high-impact polystyrene (HIPS) foams fabricated by high-pressure foam injection molding with mold opening," *Journal of Materials Chemistry C*, vol. 6, no. 45, pp. 12294–12305, 2018.

[24] J. Yu, Z. Han, Y. Beixue, and Z. Jun, "No temperature dependence of thermal conductivity of high impact polystyrene/Cu alloy composites: effective medium theory study," *Journal of Alloys and Compounds*, vol. 947, article 169519, 2023.

[25] M. Choudhury, S. Mohanty, and S. K. Nayak, "Effect of surface modification of aluminum nitride on electrical and thermal characterizations of thermosetting polymeric nanocomposites," *Composites*, vol. 34, no. 1, pp. 1–14, 2013.

[26] A. M. El Nahrawy, A. B. A. Hammad, and A. M. Youssef, "Thermal, dielectric and antimicrobial properties of polystyrene-assisted/ITO:Cu nanocomposites," *Applied Physics A*, vol. 125, no. 1, 2019.

[27] A. M. El Nahrawy, A. S. Montaser, and A. M. Bakr, "Impact of ZnO on the spectroscopic, mechanical, and UPF properties of Fe_2O_3-tough polystyrene-based nanocomposites," *Journal of Materials Science: Materials in Electronics*, vol. 32, pp. 28019–28031, 2021.

[28] N. El, M. H. Amany, B. Ali, S. Ahmed, M. Tharwat, and E. Abd, "Sol–gel synthesis and physical characterization of high impact polystyrene nanocomposites based on Fe_2O_3 doped with ZnO," *Applied Physics A*, vol. 126, no. 8, 2020.

[29] Q. Tarrés, H. Oliver-Ortega, F. X. Espinach, P. Mutjé, M. Delgado-Aguilar, and J. A. Méndez, "Determination of mean intrinsic flexural strength and coupling factor of natural fiber reinforcement in polylactic acid biocomposites," *Polymers*, vol. 11, no. 11, p. 1736, 2019.

[30] N. Sapiai, A. Jumahat, M. Jawaid, M. Midani, and A. Khan, "Tensile and flexural properties of silica nanoparticles modified unidirectional kenaf and hybrid glass/kenaf epoxy composites," *Polymers*, vol. 12, no. 11, p. 2733, 2020.

[31] M. Asimina, G. Matthieu, and S. Constantinos, "Tensile and flexural behaviour of a graphene/epoxy composite: experiments and simulation," *Journal of Physics: Materials*, vol. 3, no. 1, article 014006, 2020.

[32] F. R. Khalidi and M. A. Rajab, "Hardness and wear resistance of composite materials supported by graphite and silica particles and reinforced by cuffler fiber," *American Journal of Engineering Research*, vol. 7, no. 11, pp. 317–322, 2018.

[33] S. Hachani, A. Meghezzi, N. Nadia, and M. Slimani, "Impact of magnesium oxide incorporation on tensile and hardness properties of polystyrene/magnesium oxide composites," *Journal of Chemical and Pharmaceutical Sciences*, vol. 9, no. 4, pp. 2664–2667, 2016.

[34] W. Guanglei, W. Yiqun, W. Kuikui, and F. Ailing, "The effect of modified AlN on the thermal conductivity, mechanical and thermal properties of AlN/polystyrene composites," *RSC Advances*, vol. 6, no. 104, pp. 102542–102548, 2016.